Decentralized Finite Control Set Model Predictive Control Strategy of Microgrids for Unbalanced and Harmonic Power Management

Zhuoli Zhao[1], (Member, IEEE), Jiexiong Zhang[1], Baiping Yan[1], (Member, IEEE), Runting Cheng[1], Chun Sing Lai[1,2], (Senior Member, IEEE), Liping Huang[1], (Student Member, IEEE), Quanxue Guan[3], (Member, IEEE) and Loi Lei Lai[1], (Fellow, IEEE)

[1]School of Automation, Guangdong University of Technology, Guangzhou 510006, China
[2]Brunel Institute of Power Systems, Department of Electronic & Computer Engineering, Brunel University London, London, UB8 3PH, UK
[3]Department of Electrical and Electronics Engineering, University of Nottingham, Nottingham, NG7 2RD, UK

Corresponding authors: Loi Lei Lai (l.l.lai@gdut.edu.cn) and Baiping Yan (d_enip@163.com).

ABSTRACT In this paper, a modified decentralized finite control set model predictive control (FCS-MPC) scheme for the distributed energy resources (DERs) is proposed to improve the power management quality of the prosumers integrated microgrids under the condition of harmonic and unbalance loads. The proposed control strategy for the microgrids mainly consists of the power droop controller, the model predictive controller delay compensation, feedback correction and the unbalance compensation mechanism. The feedback correction method is used to correct the delay compensation, which effectively reduces the average switching frequency (ASF) and voltage total harmonic distortion (THD). By sharing the negative sequence reactive power of the microgrid, power distribution between the prosumers' DERs is improved. The DERs in the prosumers can be integrated without any communication wire. The transient response and robustness to parameter changes are far superior to hierarchical cascaded control. Moreover, the proposed control strategy can better suppress harmonic and reduce and share fundamental negative sequence reactive power under microgrid unbalance and nonlinear load conditions. Finally, the effectiveness of the proposed FCS-MPC control strategy is validated by time-domain simulation results and real-time tests with RT-Lab under the condition of unbalanced and nonlinear loads in the microgrids.

INDEX TERMS Microgrids, finite control set (FCS), model predictive control (MPC), voltage source converter (VSC), unbalance and harmonics control.

I. INTRODUCTION

With the development of the global economy and society, the use of fossil energy has caused a series of environmental problems. The growing demand for renewable energy (RES) has led to the increasing penetration of distributed generation (DG) units in the power systems, such as solar, wind, tidal and fuel cells [1]–[5]. Generally, various types of DG systems can be connected to the microgrid to improve the flexibility and reliability of the distribution network system. [6]–[8]. Microgrids are an effective method to solve the high penetration rate of renewable energy in the future smart grid [9]–[12].

In general, the ac microgrid facilitates deployment and compatibility with existing equipment. For the centralized control structure, the control of all units relies on by a dedicated central controller, which requires extensive communication between the central controller and the controlled units. The high reliance of data acquisition and supervisory control on communication not only makes deploying new DGs cumbersome but also results in the security issues of the communication failure [13]–[15].

On the other hand, decentralized control structure eliminates the need for complicated communication network for data transmission within the microgrids. In this case,

droop control strategies and their variants are the universal choices [16], [17]. In the islanded microgrid, the active power and reactive power sharing among the DG units can be achieved by adopting the P-f/Q-E droop control method with only local information [18], [19]. However, the traditional droop control approach cannot effectively cope with the harmonic voltage and negative sequence voltage when nonlinear loads or unbalance loads connected to the microgrids [20], [21]. In order to overcome these issues and address the harmonic and unbalanced power sharing in microgrids, improved droop control approaches are proposed in [22]–[24]. In [22], a dynamic consensus algorithm is adopted to realize the negative sequence current sharing to compensate the unbalance effectively. [23] proposes an adaptive virtual impedance control method based on injecting a very small ac signal (SACS) into the output voltage of each inverter. The droop method is used to adjust the virtual impedance, thereby adjusting the distribution of unbalance and harmonic power in the microgrid system. In [24], an auxiliary controller is supplemented to the cascaded hierarchical control scheme of an islanded microgrid to enhance the unbalance and harmonics control and obtain accurate power sharing. In [25] and [26], the enhancement of the voltage quality of critical load bus in microgrids are studied. In [25], low-bandwidth communication (LBC) technology is used to send appropriate signals of the secondary control from the microgrid control center to the primary control; thus, the voltage unbalanced compensation can be achieved. In [26], a complementary part is added to the secondary control loop to limit the voltage unbalance factor at local buses and DG terminals.

However, the conventional cascaded control structure presented in [20]–[26] has inherent drawbacks such as slow response speed, which will dramatically degrade the effect of the compensated and improved control schemes in hierarchical control architecture. Therefore, the main issues associated with the nonlinearity of the loads and dc dynamics will deteriorate the power quality of the voltage source converter (VSC) based microgrids.

Model predictive control (MPC) which was originally applied to industrial process control has many attractive features: 1) dealing with multivariate control problems; 2) easy to adjust; 3) explicitly considering constraints [27], [28]. With the development of digital processor technology, model predictive control is gradually applied to power converters and drivers [29], [30], such as motor driver [31], [32], uninterrupted power supply (UPS) [33], static compensator [34], [35]. Recently, MPC has been applied to microgrids, providing a new solution for the control of grid-connected inverters. In [36], a continuous control set model predictive control (CCS-MPC) method is introduced for grid-connected inverters. In [37], MPC is combined with the droop control method, which is used to minimize voltage unbalance, improve current limiting and prevent overload of active power. In [38], a cost function-based CCS-MPC is proposed to compensate the voltage imbalance and different harmonics of the power grid. However, when CCS-MPC is applied to the grid-connected inverters, the compensation for harmonics and unbalance will bring a substantial calculation burden. Moreover, the non-ideality characteristics of the inverters will bring more challenges to the modeling and control process.

On the other hand, the finite control set model predictive control (FCS-MPC) is easy to implement and has low computational cost. The FCS-MPC method can predict the future behavior of system control variables under finite switching conditions. The preset cost function defines the weight of different control variables (such as voltage, current, switching frequency) in the control target. This feature provides new options for improving power quality.

Nevertheless, the variable switching frequency of this control method will lead to more harmonics for the converters. In [39]–[46], the finite control model predictive control is applied to the grid-connected inverter, and the results show that MPC is superior to traditional controllers in terms of steady-state and transient response. In [41], a FCS-MPC is developed that does not require tuning and has low computational burden. [42] proposes a hybrid control strategy of FCS-MPC and deadbeat control to achieve a fixed frequency and robustness. In [43], a FCS-MPC is applied to photovoltaic power generation, which realizes maximum power tracking and voltage and frequency control on the ac bus. In [44], a decentralized FCS-MPC achieves excellent dynamic characteristics and robustness. [45] provides a method to test the stability of FCS-MPC. In [46], a FCS-MPC based microgrid control scheme is presented considering limitation of fault current and smooth transition between islanded and grid-connected modes.

It should be noted that nonlinear and unbalance loads are typical loads in residential microgrids. In [47], a cost function-based finite control set model predictive control method is used to implement unbalance compensation for grid mode operation. However, the studies mentioned above have not considered the harmonic compensation and unbalance control in islanded microgrids when adopting FCS-MPC. Therefore, there is a research gap in developing the FCS-MPC control strategy for islanded microgrids under unbalanced and harmonic load conditions.

In this paper, a decentralized FCS-MPC control strategy for the VSC-based islanded microgrids in the case of unbalanced and nonlinear loads is proposed. Feedback correction is used to reduce prediction errors and switching times, thereby reducing voltage distortion. An unbalance compensation is proposed, which reduce and share fundamental negative sequence reactive power. The numerical simulation was implemented under the condition of unbalanced and nonlinear loads using MATLAB/Simulink tools, and real-time verification testing was performed with RT-Lab. The effectiveness of the proposed control strategy was verified.

The key contributions of this paper are highlighted as follows:

1) A modified decentralized FCS-MPC control framework is proposed to reduce the harmonics of the microgrid and
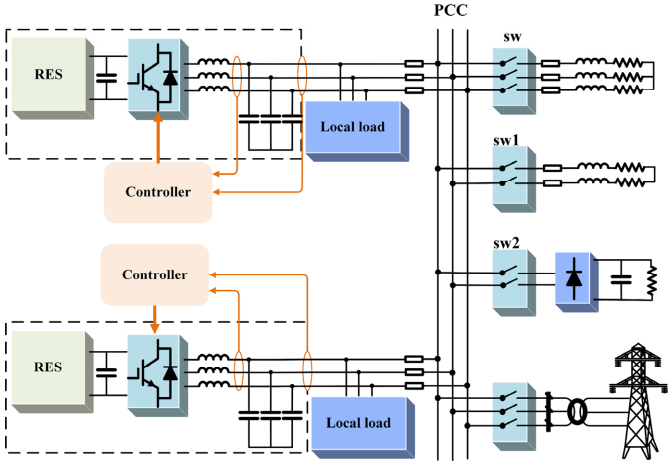
FIGURE 1. Structure of microgrid with multiple parallel-connected DG units.

TABLE I
OUTPUT VOLTAGE VECTOR OF THE VSC

S_a	S_b	S_c	V_α	V_β
0	0	0	0	0
0	0	1	$-V_{dc}/3$	$-\sqrt{3}V_{dc}/3$
0	1	0	$-V_{dc}/3$	$\sqrt{3}V_{dc}/3$
0	1	1	$-2V_{dc}/3$	0
1	0	0	$2V_{dc}/3$	0
1	0	1	$V_{dc}/3$	$-\sqrt{3}V_{dc}/3$
1	1	0	$V_{dc}/3$	$\sqrt{3}V_{dc}/3$
1	1	1	0	0

FIGURE 2. Structure of the grid-connected DG units.

share negative sequence reactive power between distributed energy resources (DERs).

2) A feedback correction method for FCS-MPC is proposed to improve delay compensation and output vector prediction, thereby improving voltage tracking and control of voltage harmonics.

3) Compared with conventional FCS-MPC, the proposed modified decentralized FCS-MPC strategy improves the robustness of circuit parameter changes, thereby reducing the dependence on model matching.

The rest of this paper is organized as follows. In Section II, the discrete dynamic model of VSC DG units is presented. Section III proposes the decentralized FCS-MPC strategy. In Section IV, the numerical simulation is implemented using MATLAB/ Simulink tools. In Section V, real-time verification testing is performed with RT-Lab. Section VI gives the conclusion.

II. DISCRETE DYNAMIC MODELING OF VSC DG UNITS

As shown in Fig. 1, the studied microgrid in this paper consists of several parallel VSC DG units, which are connected to the point of common coupling (PCC) through corresponding feeders respectively. The DG is composed of renewable energy source (RES), a three-phase inverter and an LC filter. Note that the studied microgrid in Fig. 1 is a three-phase three-wire system. Therefore, zero-sequence current is not considered in this paper.

A. VSC DG MODEL

As shown in Fig. 2, the inverter is connected to the microgrid via LC filter. The output voltage vector of the three-phase inverter in the αβ stationary orthogonal reference frame is given in Table I. In Table I, S_a, S_b and S_c are the switch configurations of phases A, B and C, respectively. The LC filter is connected to the outlet of the inverter and is three-phase symmetrical. The dynamic characteristics of the filter inductance L_f in complex αβ frame can be described as:

$$L_f \frac{di_{la}}{dt} = -r_f i_{la} + v_{i\alpha} - v_{o\alpha} \quad (1)$$

$$L_f \frac{di_{l\beta}}{dt} = -r_f i_{l\beta} + v_{i\beta} - v_{o\beta} \quad (2)$$

where i_l is the current of the filter inductance; r_f is the resistance of the filter inductance; v_i is the output voltage of the inverter; v_o is the voltage of the filter capacitor C_f.

The dynamic characteristics of the filter capacitor C_f in complex αβ frame can be described as:

$$C_f \frac{dv_{o\alpha}}{dt} = i_{l\alpha} - i_{o\alpha} \quad (3)$$

$$C_f \frac{dv_{o\beta}}{dt} = i_{l\beta} - i_{o\beta} \quad (4)$$

where i_o is output current of the LC filter.

Thus, the state space equations of the VSC with an LC filter can be obtained by combining (1)–(4), which is expressed as follows:

$$\frac{d}{dt}\mathbf{x} = \mathbf{A}\mathbf{x} + \mathbf{B}\mathbf{y} \quad (5)$$

where

$$\mathbf{x} = \begin{bmatrix} i_l \\ v_o \end{bmatrix}, \ \mathbf{y} = \begin{bmatrix} v_i \\ i_o \end{bmatrix}, \ \mathbf{A} = \begin{bmatrix} -\frac{r_f}{L_f} & -\frac{1}{L_f} \\ \frac{1}{C} & 0 \end{bmatrix}, \ \mathbf{B} = \begin{bmatrix} -\frac{1}{L_f} & 0 \\ 0 & \frac{1}{C} \end{bmatrix}$$

B. DISCRETIZATION OF THE DG DYNAMIC MODEL

Discretization of continuous state space equation is necessary for the digital controller in practical applications. In this paper, because of the advantage of the accurate approximation between continuous and discrete systems, the zero-order hold (ZOH) discretization method is adopted for the discretization of the DG dynamic model. The discretization equation is used to predict the output of the inverter. Hence, Equation (5) can be discretized as follows:

$$\mathbf{x}(k+1) = \mathbf{A_d}\mathbf{x}(k) + \mathbf{B_d}\mathbf{y}(k) \quad (6)$$

where $\mathbf{x}(k+1)$ are the predicted current of the filter inductance $i_f(k+1)$ and the voltage of the filter capacitor $v_f(k+1)$ at the time of $(k+1)$T, respectively; $\mathbf{x}(k)$ are the current of the filter inductance $i_f(k)$ and the voltage of the
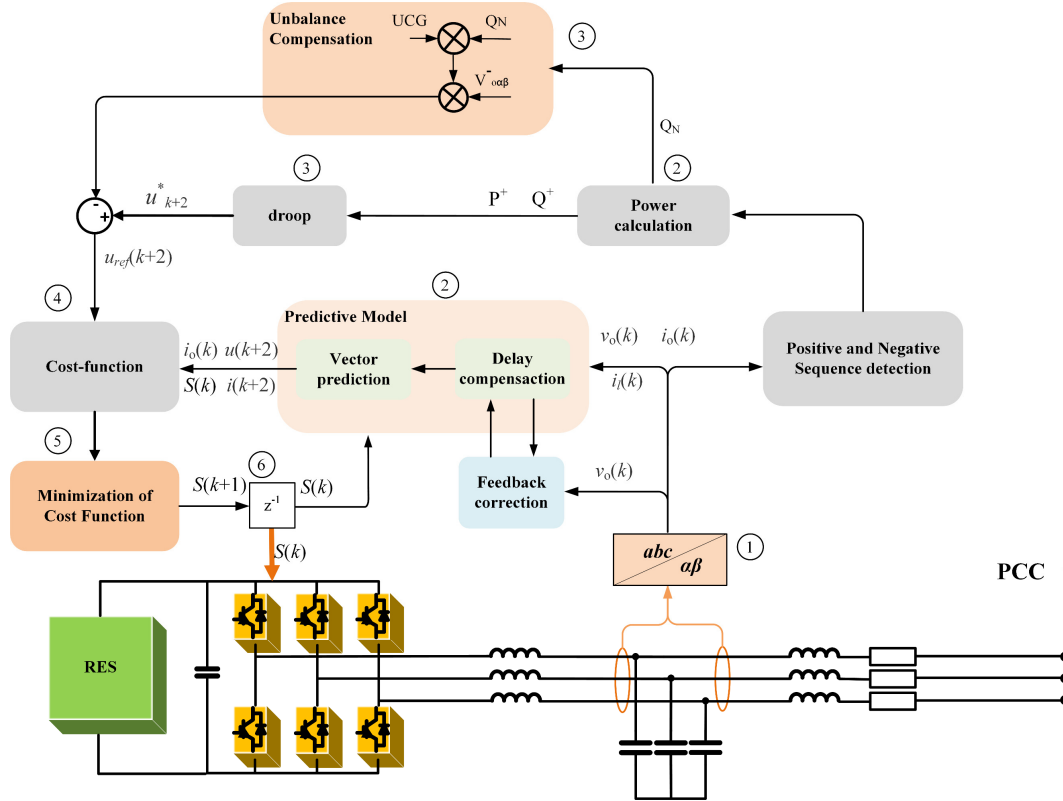
FIGURE 3. Diagram of the proposed modified decentralized FCS-MPC strategy for the islanded microgrid.

filter capacitor $v_f(k)$ at the time of kT; $y(k)$ are the output voltage of inverter and output current of LC filter at the time of kT. A_d and B_d can be calculated by:

$$A_d = e^{AT_s} \qquad (7)$$

and

$$B_d = \int_0^{T_s} e^A B dt \qquad (8)$$

where T_s is the sampling time of the controller.

III. PROPOSED MODIFIED DECENTRALIZED FCS-MPC CONTROL STRATEGY FOR MICROGRIDS

As shown in Fig. 3, the proposed control strategy is comprised of two parts: the harmonic compensation and the unbalance compensation based on FCS-MPC. The harmonic compensation function is achieved by a supplement of feedback correction in the FCS-MPC cost function. The unbalance compensation is implemented by the auxiliary loop, which uses the fundamental negative sequence reactive power to change the output reference voltage. The voltage and current signals of the VSC DG are sampled and feed to the FCS-MPC strategy, and then provide switching signals to the inverter.

A. POSITIVE/NEGATIVE SEQUENCE POWER CALCULATION

The fundamental positive sequence and fundamental negative sequence current of the DG unit are separated by using the second-order generalized integrator, which are detailed in

Section III-F. Then, the active power P^+, reactive power Q^+ and unbalance power Q^- of the DG unit can be expressed as follows [48]:

$$P^+ = V_\alpha \cdot I_\alpha^+ + V_\beta \cdot I_\beta^+ \qquad (9)$$

$$Q^+ = V_\beta \cdot I_\alpha^+ - V_\alpha \cdot I_\beta^+ \qquad (10)$$

$$Q^- = E^* \cdot \sqrt{(I_\alpha^-)^2 + (I_\beta^-)^2} \qquad (11)$$

where I^+ is the fundamental positive sequence current of the DG unit; I^- is the fundamental negative sequence current of the DG unit; E^* is the nominal voltage.

B. DROOP CONTROL

Positive sequence active power-frequency and positive sequence reactive power-voltage droop control method are used for power sharing among the DG units, while avoid using the communication wire.

$$V_{ref} = V_{nom} - m\widetilde{Q} \qquad (12)$$

$$\omega_{ref} = \omega_{nom} - n\widetilde{P} \qquad (13)$$

where V_{ref} is the reference voltage amplitude, ω_{ref} is the reference frequency, V_{ref} is the system nominal voltage amplitude, ω_{nom} is the system nominal frequency. $\widetilde{P}$ and $\widetilde{Q}$ are the active power and reactive power of the DG unit, which can be calculated by

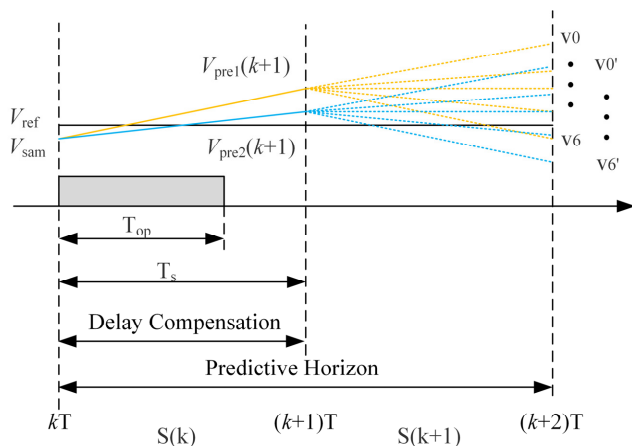$$\widetilde{P} = \frac{\omega_c}{s + \omega_c} P^+ \qquad (14)$$

FIGURE 4. Analysis of the feedback correction.

$$\widetilde{Q} = \frac{\omega_c}{s+\omega_c} Q^+ \qquad (15)$$

where ω_c is the cut-off frequency of the low pass filter.

C. MODIFIED FINITE CONTROL SET MODEL PREDICTIVE CONTROL SCHEME

In order to further reduce the computational burden and to simplify the analysis, this paper considers a one-step prediction in the FCS-MPC strategy. At the beginning of each control cycle, the controller simultaneously samples the system state variables and switches the system.

In actual application, considering the calculation time and sampling time of the controller cannot be neglected, the FCS-MPC strategy is performed in the following steps to compensate for the delay time. Firstly, the current of the filter inductor i_l, the voltage of the filter capacitor V_c and the output current I_o at kT are measured. And then, the state variables at $(k+1)$T with the compensation of the controller delay are predicted according to the output voltage vector V_i and Equation (6). Secondly, the output of the LC filter for all candidate voltage vectors in the FCS at the $(k+2)$T sampling instant are predicted. Finally, using the proposed cost-function, the predicted results of each voltage vector are evaluated. Then the corresponding switch state will be selected from all candidate voltage vectors, which can minimize the cost function J.

It should be noted that the cost function value represents the deviations between the control result and the object. In addition, the weights of different control targets in the control process are defined in the cost function, so that users can intuitively optimize the control targets [28]. In this work, the proposed cost function is expressed as follow:

$$J = J_v + \lambda_{der} J_{der} + \lambda_{sw} J_{sw} + i_{lim} \qquad (16)$$

where J_v is the predicted voltage tracking error, J_{der} is the voltage differential term and J_{sw} is the penalty for switching effort. λ_{der} and λ_{sw} are the corresponding associated weighting factors. It should be noted that simplifying the weighting factors into λ_{der} and λ_{sw} can facilitate analysis and tuning while reducing the amount of calculations in the processor. i_{lim} is the constraint of inverter output current, if $i_l > i_{max}$, $i_{lim} = \infty$; else, $i_{lim} = 0$. i_{max} is the maximum output current of the inverter.

In (16), the predicted voltage tracking error term can be defined as follows:

$$J_v = (V_{ref} - V)^2 \qquad (17)$$

where V_{ref} is the reference voltage vector, V is the predicted output voltage at $(k+2)$T.

In the second-order systems of VSC with LC filter, the tracking of voltage and voltage derivatives allows the system to be effectively controlled, which is more satisfactory than the tracking control effect only by voltage. The capacitor reference voltage is defined as follows:

$$v_\alpha^* = V_{ref}\sin(\omega_{ref}\, t)$$
$$v_\beta^* = V_{ref}\cos(\omega_{ref}\, t) \qquad (18)$$

The derivative of the capacitor reference voltage is:

$$\frac{dv_\alpha^*}{dt} = \omega_{ref}V_{ref}\cos(\omega_{ref}\, t) = \omega_{ref}v_\beta^*$$
$$\frac{dv_\beta^*}{dt} = -\omega_{ref}V_{ref}\sin(\omega_{ref}\, t) = -\omega_{ref}v_\alpha^* \qquad (19)$$

The derivative of the capacitor voltage through the dynamic characteristics of the capacitor is:

$$\frac{dv_{o\alpha}}{dt} = \frac{i_{l\alpha} - i_{o\alpha}}{C_f}$$
$$\frac{dv_{o\beta}}{dt} = -\frac{i_{l\beta} - i_{o\beta}}{C_f} \qquad (20)$$

The tracking error of the capacitor voltage differential can be obtained by subtracting Equation (20) from Equation (19). In order to facilitate computer operation, the capacitor C_f is multiplied on both sides.

$$J_{der} = \left(\omega_{ref}C_f v_\beta^* - i_{l\alpha} + i_{o\alpha}\right)^2 + \left(\omega_{ref}C_f v_\alpha^* + i_{l\beta} - i_{o\beta}\right)^2 \qquad (21)$$

The penalty item for switching J_{sw} can reduce switch frequency which can be calculated by:

$$J_{sw} = \frac{\sum_{i=a,b,c}|S_i(k+1) - S_i(k)|}{3*2} \qquad (22)$$

where S_i is the switch configuration of phase A, B and C.

D. FEEDBACK CORRECTION

The measures to reduce the tracking error can be achieved not only by the constraints on the cost function, but also by reducing the prediction error. As shown in Fig. 4, in delay compensation, prediction result with small differences may make a different choice of optimal switching state, such as $V_{pre1}(k+1)$ and $V_{pre2}(k+1)$. Therefore, reducing the prediction error of delay compensation will effectively reduce the tracking error and the resulting oscillations and harmonics. Compared with the control period, the fundamental periodic error changes slowly, which can be approximated as:

$$v_{err}(k+1) = v_{pre}(k) - v_{sam}(k) \qquad (23)$$

where $v_{sam}(k)$ is the sampling value of capacitor voltage at kT; $v_{pre}(k)$ is the predicted value of the capacitor voltage at kT from the last control cycle. Therefore, the correction value of the predicted voltage used for delay compensation can be expressed as:

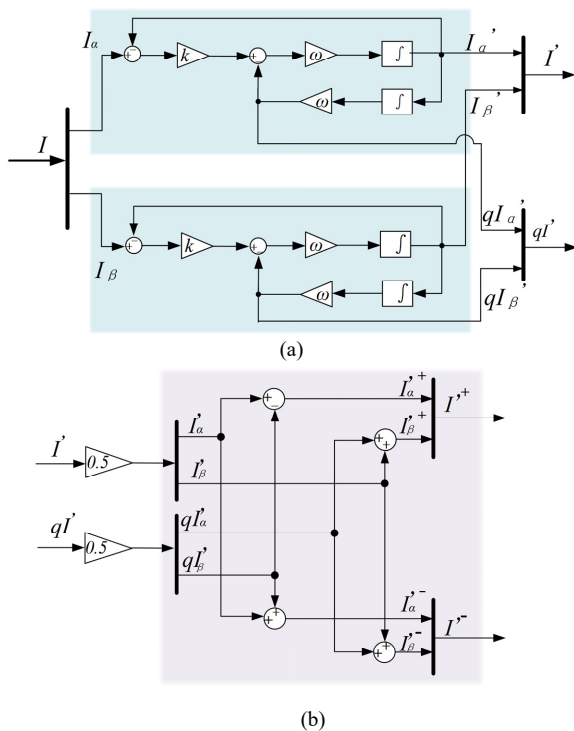$$v_{cor}(k+1) = v_{pre}(k+1) - \lambda_C v_{err}(k+1) \qquad (24)$$

(a)

(b)

FIGURE 5. Sequence extraction block diagram. (a) DSOGI-QSG (b) PNSC.

where $v_{pre}(k+1)$ is the predicted voltage calculated by the discrete model, λ_c is the feedback correction coefficient.

E. UNBALANCE COMPENSATION METHOD

When the load is unbalanced, the voltage unbalance can be compensated by reducing the negative sequence voltage. As shown in Fig. 3, the compensation reference can be obtained by the product of the negative reactive power Q^-, an unbalance compensation gain (UCG), and the fundamental negative-sequence voltage v_o^-. With the compensation proceeds, Q^- gradually decreases. Also, the compensation efforts will be reduced, helping microgrids to distribute compensation efforts properly. The adjustment of the constant UCG needs to consider the compensation effect of unbalance.

F. SEQUENCE EXTRACTION

For the calculation of the DG output power, the output current of the DG is extracted by using a dual second-order generalized integrator quadrature signal generator (DSOGI-QSG) and the positive-negative-sequence calculation (PNSC) block, which has fast dynamic response and high accuracy. The implementation of sequence extraction is shown in Fig. 5.

In Fig. 5, k is the coefficient of the bandwidth of the SOGI-QSG; ω is the resonant frequency. The output I^+ and I^- is the positive and negative sequence current in $\alpha\beta$ frame.

IV. SIMULATION RESULTS

The proposed FCS-MPC control strategy is implemented in an islanded ac microgrid consisting of two VSC DG units, which helps simplify the analysis in this study. The

TABLE II
MICROGRID PARAMETER

| System Parameter	Value
Nominal voltage	V_{nom} = 380 V
System nominal frequency	f_{nom} = 50 Hz
Nominal power of the DGs	S_{nom} = 10 kVA
DC link voltage	V_{dc} = 650 V
Resistance of filter inductor	r_L = 0.1 Ω
Inductance of filter	L_f = 1.35 mH
Capacitance of filter	C_f = 50 μF
Resistance of line	r_{line} = 0.1 Ω
Inductance of line	L_{line} = 2.4 mH
Droop coefficients	m = 0.001 rad/s/W, n = 0.0001 V/VAr
Weighting coefficients	λ_{der} = 0.1, λ_{sw} = 3, λ_c = 1
Sampling time	T_s = 20 μs
Unbalance compensation gain	UCG = 1e-4
Load Parameter	**Value**
Unbalance load	R_u = 80 Ω
Nonlinear load	C = 2200 μF, R = 50 Ω

(a)

(b)
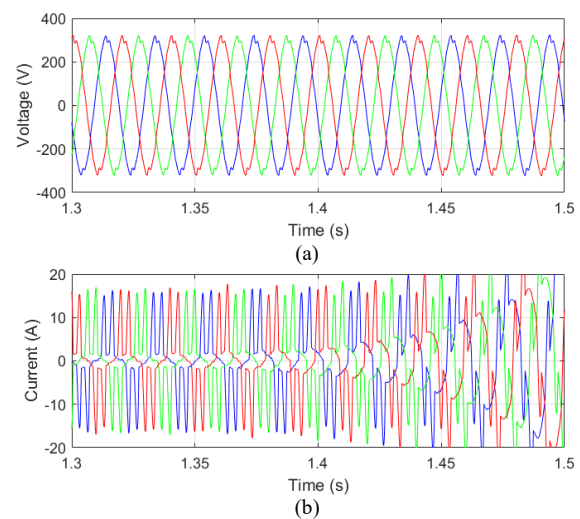
FIGURE 6. System response of the microgrid with the conventional cascaded PI method under nonlinear load. (a) Output voltage waveforms of DG1. (b) Output current waveforms of DG1.

microgrid is established for time-domain simulation in MATLAB/Simulink environment. As shown in Fig. 1, an unbalanced load and a nonlinear load are connected to the microgrid via the switches sw1 and sw2, respectively. Thus, the proposed control strategy can be verified under complex load conditions, including nonlinear and unbalanced loads. The main parameters of the islanded ac microgrid are given in Table II.

A. PERFORMANCE UNDER THE CONDITION OF NONLINEAR LOAD

As shown in Fig. 1, the nonlinear load is a three phases diode rectifier with a parallel RC load connected to the PCC. The comparison of the microgrid performance of the conventional cascaded PI method, the conventional proportional resonant (PR) control method and the proposed modified decentralized FCS-MPC control strategy under the condition of nonlinear load are shown in Figs. 6-8, respectively.

In this operating case, two fundamental periods of the capacitor voltage are sampled with a sampling time of 1 μs.
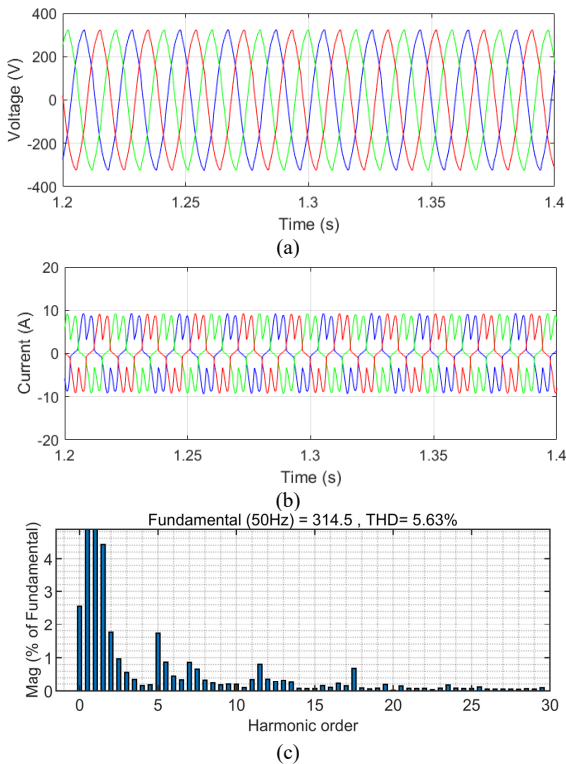
FIGURE 7. System response of the microgrid with the conventional PR method under nonlinear load. (a) Output voltage waveforms of DG1. (b) Output current waveforms of DG1. (c) FFT analysis of phase A.
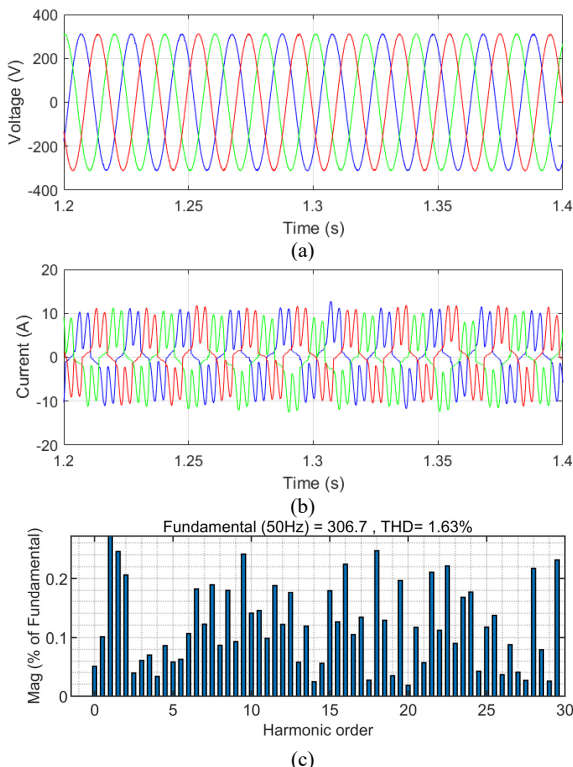

FIGURE 8. System response of the microgrid with the proposed modified decentralized FCS-MPC strategy under nonlinear load. (a) Output voltage waveforms of DG1. (b) Output current waveforms of DG1. (c) FFT analysis of phase A.

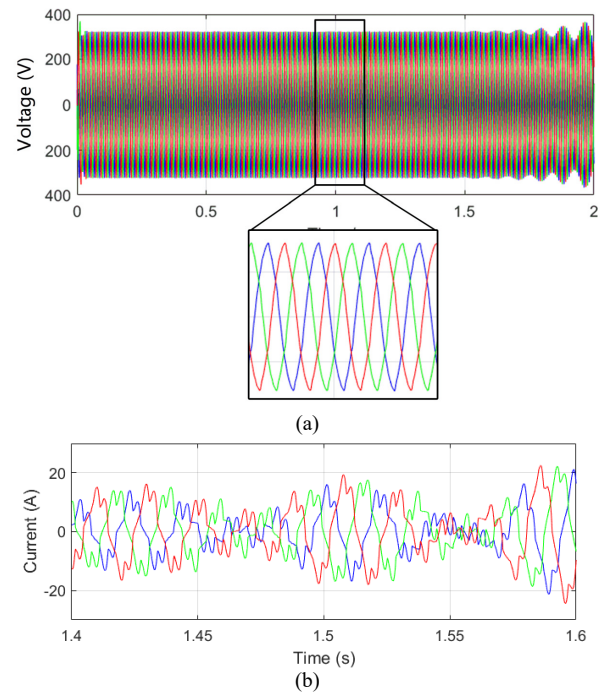Then, in order to identify individual harmonic amplitudes,

FIGURE 9. System response of the microgrid with conventional PR method under unbalanced and nonlinear loads. (a) Output voltage waveforms of DG1. (b) Output current waveforms of DG1.

the signal is processed using the Fast Fourier Transform (FFT) algorithm provided in the MATLAB.

It can be seen from voltage and current waveforms of the DG unit in Fig. 6 that, under the condition of nonlinear load, the microgrid using the conventional cascaded PI control method appears a severe distortion of the output voltage waveform. Moreover, the output current of the DG unit cannot be effectively controlled. The microgrid system loses stability and diverges gradually.

The voltage and current waveforms of the DG unit when using the conventional PR control method and the proposed modified decentralized FCS-MPC control strategy are shown in Fig. 7 and Fig. 8, respectively. Obviously, the output voltage of the DG unit which uses the proposed control strategy presents better sinusoidal. Due to the nonlinear characteristics of the V/I relationship of the diode, the output voltage of the DG based on conventional PR control has significant distortion, and the corresponding total harmonic distortion (THD) is 5.63 %. At the same time, relatively good harmonic currents are shared between the DG units. It can be observed from the diagram of the FFT analysis that the output voltage distortion of DG using traditional cascaded PR control is mainly concentrated on odd harmonics.

As shown in Fig. 8, due to the fast response of FCS-MPC and the reduction of the prediction error by the feedback correction method, the proposed modified decentralized FCS-MPC strategy is well capable of achieving excellent suppression effect on each order harmonic. It can be seen from Fig. 8 (c) that when using the proposed modified decentralized FCS-MPC control strategy, the output voltage THD of the DG is 1.63 %. Compared with the conventional PR control method
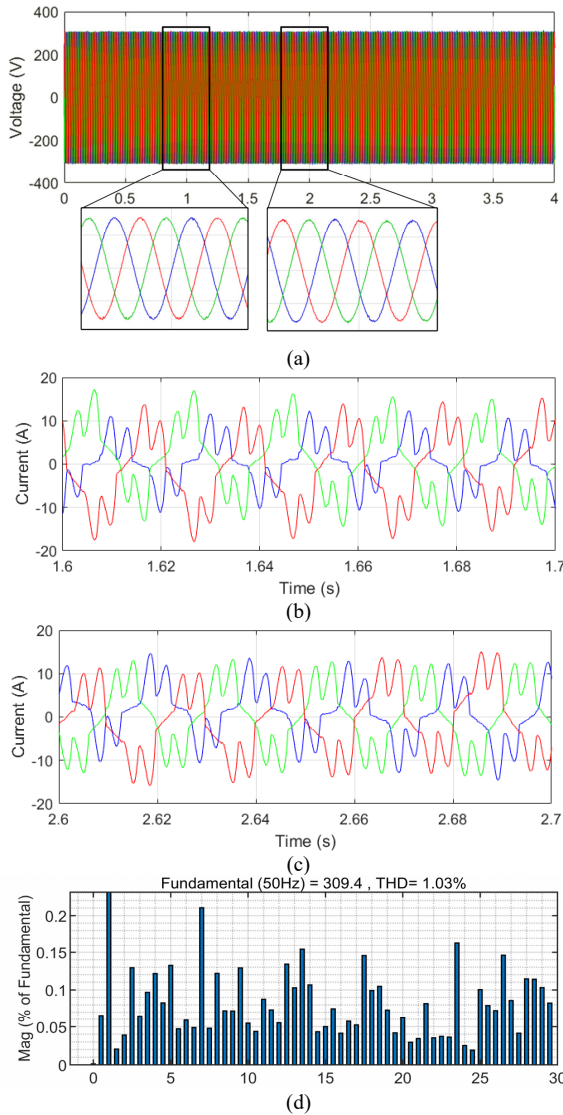
FIGURE 10. System response of the microgrid with the proposed modified decentralized FCS-MPC strategy under unbalanced and nonlinear loads. (a) Output voltage waveforms of DG1. (b) Output current waveforms of DG1 before compensation. (c) Output current waveforms of DG1 after compensation. (d) FFT analysis of phase A.

FIGURE 11. System response of the microgrid with the proposed modified decentralized FCS-MPC strategy under unbalanced and nonlinear loads. (a) Output fundamental positive sequence active power. (b) Output fundamental negative sequence reactive power.

FIGURE 12. System response of the microgrid with the PR control method under step load. (a) Output voltage waveforms of DG1. (b) Output current waveforms of DG1.

shown in Fig. 7 (c), the harmonics can be significantly reduced with the proposed control strategy. The feature in Fig. 8 shows excellent performance of the proposed method under nonlinear load condition.

B. PERFORMANCE UNDER THE CONDITION OF UNBALANCED AND NONLINEAR LOADS

In order to test the validity of the proposed modified decentralized FCS-MPC strategy in a VSC based microgrid with generalized loads, a nonlinear load and an unbalanced load are connected to the PCC at t=0 s and t=1 s , respectively. Thus, sw2 and sw1 switch to the closed states.

The system performance of the microgrid adopting only the conventional PR control method is presented in Fig. 9. As can be observed from Fig. 9, the microgrid system operates stably using the conventional PR control method under only nonlinear load. After an unbalanced load is added at t=1 s, the
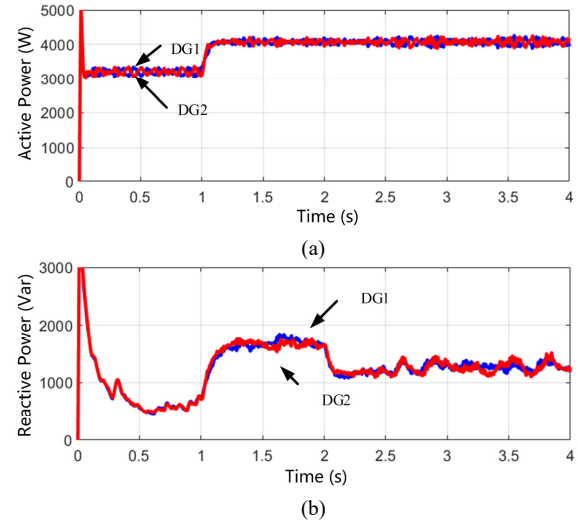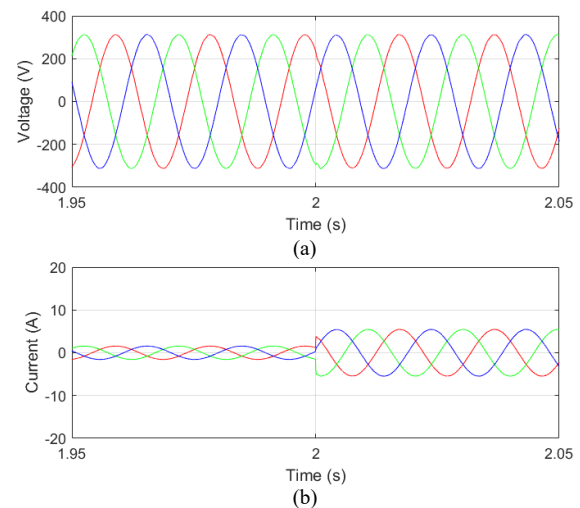
voltage and current waveforms of the DG unit start to fluctuate, and the microgrid system is gradually unstable.

In order to improve the system performance under unbalanced and nonlinear loads conditions, the proposed modified decentralized FCS-MPC strategy is adopted, and the response of the voltage, current, fundamental negative sequence active power, reactive power and negative power are shown in Fig. 10 and Fig. 11. The unbalance compensation of the proposed method is activated at t=2 s . Note that the unbalanced load is 80 Ω. It is obvious that the voltage can still maintain a good sinusoidal shape even after the unbalanced load is connected at t=1 s. After the unbalance compensation is implemented at t=2 s , the unbalance current gradually decreases, and the voltage can still maintain an excellent sinusoidal during this period. Furthermore, as shown in Fig. 11, the negative-sequence reactive power is effectively weakened, and it is well shared among different DG units.
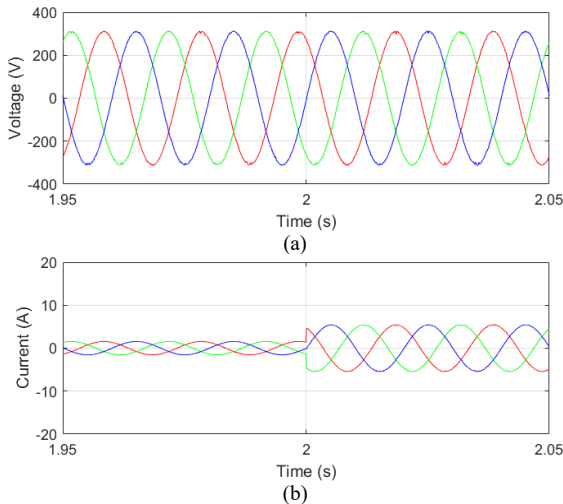
FIGURE 13. System response of the microgrid with the proposed modified decentralized FCS-MPC under step load. (a) Output voltage waveforms of DG1. (b) Output current waveforms of DG1.

Compared with the conventional PR control method in Fig. 9, it can be obviously demonstrated that the proposed modified decentralized FCS-MPC strategy provides robust performance for the microgrid under unbalanced and nonlinear loads
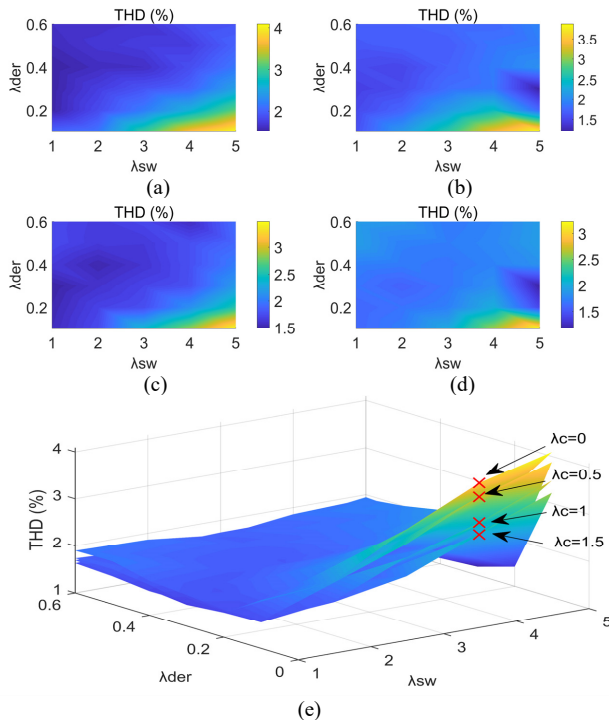

FIGURE 14. Influence of weight settings λ_{der} and λ_{sw} on the output voltage THD. (a) Without feedback correction. (b) λ_c=0.5. (c) λ_c=1. (d) λ_c=1.5. (e)The comparison of the influence of the weight setting λ_{der} and λ_{sw} on the output voltage THD.

conditions.

C. PERFORMANCE UNDER THE CONDITION OF STEP LOADS
In order to test the transient performance of the proposed modified decentralized FCS-MPC strategy in a VSC based microgrid with generalized loads, a step load (R=40 Ω) are
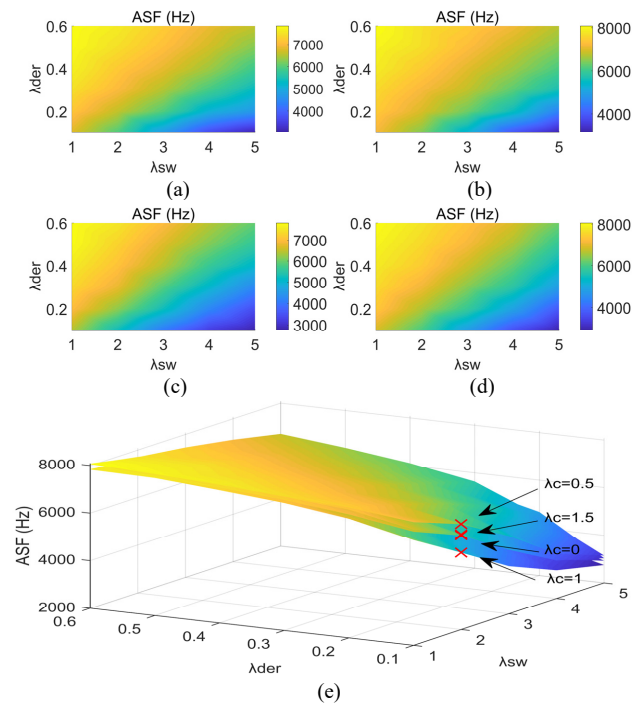

FIGURE 15. Influence of weight settings λ_{der} and λ_{sw} on the ASF. (a)Without feedback correction. (b) λ_c=0.5. (c) λ_c=1. (d) λ_c=1.5. (e)The comparison of the influence of the weight setting λ_{der} and λ_{sw} on the ASF.

connected to the PCC at t=2 s . The system response comparisons between the conventional PR control method and the proposed modified decentralized FCS-MPC control strategy are illustrated in Fig. 12 and Fig. 13, respectively. Obviously, even after a step load is connected at t=2 s, the voltage can still maintain a good sinusoidal shape, and at the same time, the current increases rapidly in response to load changes. However, some distortions generated by the voltage waveform under the PR control method indicate that the transient response of the proposed modified decentralized FCS-MPC strategy is better than the PR control.

D. CONTROL PARAMETERS AND STEADY-STATE ANALYSIS
To evaluate the switching frequency of FCS-MPC, the average switching frequency (ASF) is defined as follows:

$$f_{avg} = \frac{sw_a + sw_b + sw_c}{3 * T} \qquad (25)$$

where T=0.2 s is the calculation period of the average switching frequency. sw_a, sw_b, sw_c are the switching times of phase A, B and C, respectively in T.

In order to determine the optimal values of the key control parameters, the influence of the weighting factors λ_{der}, λ_{sw} and the feedback correction coefficient λ_c on the output voltage THD and ASF are studied with simulation results in Figs. 14 and 15. And the value of λ_{der} is varied from 0.1 to 0.6, and λ_{sw} is varied from 1 to 5, when λ_c is 0, 0.5, 1, 1.5. As shown in Fig. 14, the output voltage THD decreases as λ_{der} increases, and increases as λ_{sw} increases. The increase of feedback correction coefficient λ_c makes the control effect improve under different parameters. Furthermore, it can be
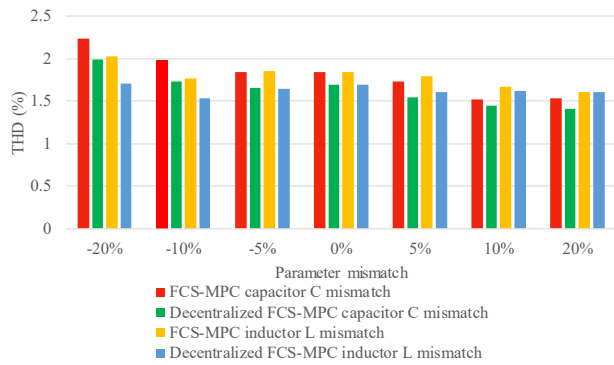
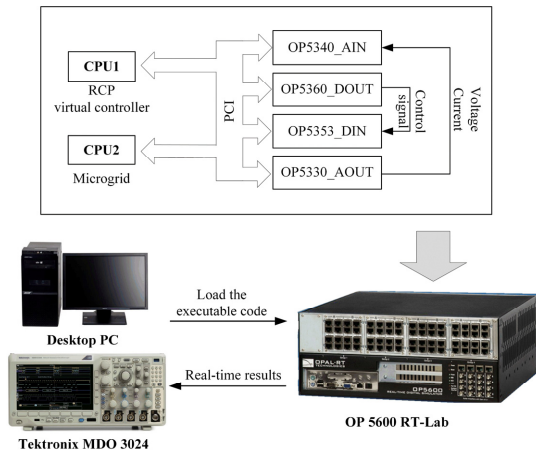**FIGURE 16.** Analysis of model parameters mismatch.

FIGURE 17. Real-time realization setup with RT-Lab.

seen from Fig. 15 that, the average switching frequency of the inverter increases with the increase of λ_{der} and decreases with the increase of λ_{sw}. Combined with the the simulation results shown in Figs. 14 and 15, the optimal values of the key control parameters λ_{der}, λ_{sw} and λ_c are selected, as presented in Table II.

E. SENSITIVITY OF THE MODEL PARAMETER VARIATION

In order to evaluate the sensitivity of the model parameters, the performance of the decentralized modified FCS-MPC in the case of capacitance or inductance mismatch was tested. The system output voltage THD with respect to parameter matching was tested when the capacitance or inductance mismatch is ±5%, ±10%, and ±20%. The simulation results are shown in Fig. 16. The decentralized modified FCS-MPC shows the robustness of matching model parameters. When the model parameters are highly mismatched, it will not significantly reduce the control effect. At the same time, the decentralized modified FCS-MPC has better control effect than conventional FCS-MPC. When the actual circuit parameters are slightly larger than the model parameters, a smaller voltage THD may be achieved. When the actual circuit parameters are slightly smaller than the model parameters, the voltage THD only slightly increases. Thus, it can be seen that the precise match of the model has no significant influence on the control effect.
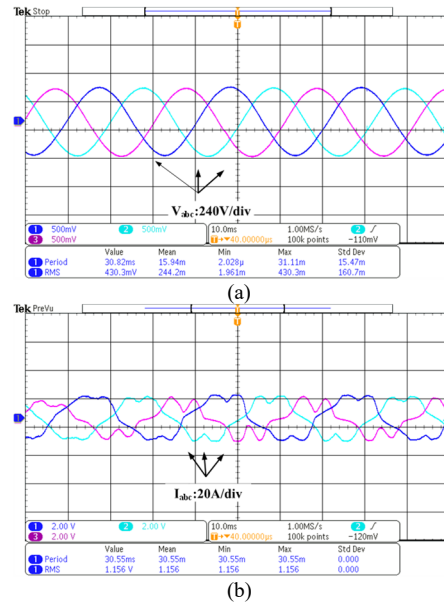
FIGURE 18. System performance with the proposed modified decentralized FCS-MPC strategy under nonlinear load. (a) Output voltage waveforms of DG1. (b) Output current waveforms of DG1.
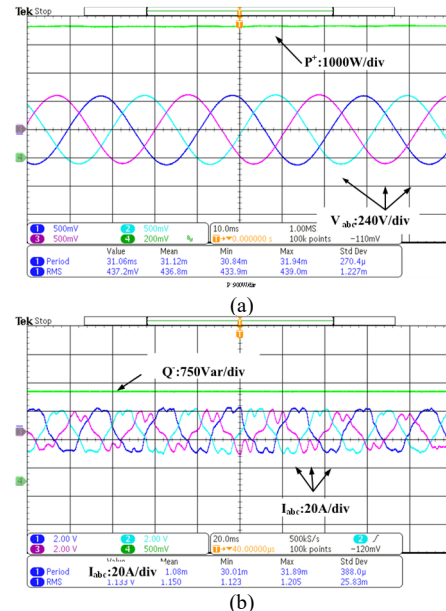
FIGURE 19. System performance with the proposed modified decentralized FCS-MPC strategy under unbalanced and nonlinear loads. (a) Output voltage waveforms and fundamental positive sequence active power of DG1. (b) Output current waveforms and fundamental negative sequence reactive power of DG1.

F. DISCUSSION

The above simulation reflects the excellent control performance of the proposed decentralized modified FCS-MPC strategy under various measures working conditions (including harmonics, unbalance and harmonics, transient step load change and parameter mismatch). The proposed decentralized modified FCS-MPC strategy mainly has the following characteristics:

(1) Under harmonic and unbalanced load conditions, the

This article has been accepted for publication in a future issue of this journal, but has not been fully edited. Content may change prior to final publication. Citation information: DOI 10.1109/ACCESS.2020.3034947, IEEE Access

Author Name: Preparation of Papers for IEEE Access

proposed decentralized modified FCS-MPC strategy has a lower THD than conventional PR and conventional FCS-MPC.

(2) The proposed modified decentralized FCS-MPC shows more robustness of modeling parameter changes than conventional FCS-MPC.

(3) Under the unbalanced load working state, the proposed modified decentralized FCS-MPC strategy can effectively share and reduce the unbalanced power.

V. REAL-TIME VERIFICATION WITH RT-LAB

In order to further verify the effectiveness of the proposed modified decentralized FCS-MPC strategy, the proposed control strategy implemented in the microgrid is verified with the real-time digital platform OP5600-OPALRT, as shown in Fig. 17. The model which is established with MATLAB/Simulink and OPAL-RT libraries is added to facilitate the real-time implementation. The implemented model in MATLAB/ Simulink is compiled with RT-LAB thus to convert the model in C-language. The loaded model in OPAL-RT is run with a sampling time of 10 us. The input/output ports of OPAL-RT are connected to the four-channel Tektronix oscilloscope MDO3024. The parameters of the microgrid system are selected to be the same with simulation, as presented in Table II. The analog signals are shown in Fig. 18 and Fig. 19.

Fig. 18 shows the voltage and current performance of the DG units using the proposed control strategy under nonlinear load. Only slight voltage distortion is observed due to the active harmonic control capability introduced by the feedback correction in the modified decentralized FCS-MPC approach. In spite of the severe nonlinear characteristics caused by the diode, the modified decentralized FCS-MPC strategy is well able to obtain a remarkable harmonic control effect. This is consistent with the simulated results in Fig. 8.

The performance of the proposed modified decentralized FCS-MPC strategy is also tested under the complex conditions of unbalanced and nonlinear loads, and the results of the output voltage, current and the negative-sequence reactive power are depicted in Fig. 19. It can be clearly observed that the voltage waveform can still maintain a sinusoidal shape. Moreover, the introduced unbalance compensation method is able to effectively suppress the negative-sequence reactive power under unbalanced loads, as shown in Fig. 19 (b). Also, these characteristics agree with the results shown in Fig. 10.

VI. CONCLUSION

This paper proposes a modified decentralized finite control set model predictive control strategy of prosumers integrated microgrids for unbalanced and harmonic power management. The proposed strategy is developed to enhance the voltage quality of the microgrids with reduced the total harmonic distortion and the load unbalance conditions. Based on the FCS-MPC strategy of the two-stage three-phase VSC, the control strategy is modified by feedback correction to suppress the harmonics of the output voltage using only one-step prediction. Compared with conventional FCS-MPC, the average switching frequency, parameter adaptability and voltage harmonics are improved. In addition, an unbalanced compensation scheme was introduced in the decentralized FCS-MPC control architecture to mitigate the impact of unbalanced loads on the DG in the microgrid. Negative sequence reactive power is well shared, and power distribution between DERs is improved. Comprehensive simulation and real-time verification with RT-Lab from a VSC microgrid have been presented to verify the effectiveness of the proposed control strategy. The obtained results show that the unbalance and harmonic are well compensated and controlled by using the proposed control technique, and the compensation effort is properly shared between the prosumers' DERs. In comparison with the conventional control method, it can be demonstrated that the proposed modified decentralized FCS-MPC strategy provides satisfactory and robust performance for practical microgrids under unbalanced and nonlinear loads conditions.

REFERENCES

[1] R. H. Lasseter, "Microgrids," *Proc. IEEE Power Eng. Soc. Winter Meet.*, Jan. 2002, vol. 1, pp. 305–308.

[2] Z. Zhao, *et al.*, "Multiple-time-scales Hierarchical Frequency Stability Control Strategy of Medium-voltage Isolated Microgrid," *IEEE Trans. Power Electron.*, vol. 31, no. 8, pp. 5974–5991, Aug. 2016.

[3] J. Rocabert, *et al.*, "Control of Power Converters in AC Microgrids," *IEEE Trans. Power Electron.*, vol. 27, no. 11, pp. 4734–4749, 2012.

[4] H. Wang, *et al.*, "A review of deep learning for renewable energy forecasting", *Energy Conversion and Management*, vol. 198, 2019.

[5] D. Xu, *et al.* "Distributed multi-energy operation of coupled electricity, heating and natural gas networks," *IEEE Transactions on Sustainable Energy*, 2020.

[6] Z. Cheng, *et al.* "A novel cascaded control to improve stability and inertia of parallel buck-boost converters in DC microgrid," *International Journal of Electrical Power & Energy Systems*, vol. 119, 105950, 2020.

[7] N. Pogaku, *et al.*, "Modeling, Analysis and Testing of Autonomous Operation of an Inverter-based Microgrid," *IEEE Trans. Power Electron.*, vol. 22, no. 2, pp. 613–625, 2007.

[8] R. H. Lasseter, "Smart Distribution: Coupled Microgrids," *Proc. IEEE*, vol. 99, no. 6, pp. 1074–1082, 2011.

[9] V. V. S. N. Murty and A. Kumar, "Multi-objective energy management in microgrids with hybrid energy sources and battery energy storage systems", *Prot Control Mod Power Syst*, vol. 1, pp.1-20, 2020.

[10] H. Wang, *et al.*, "Taxonomy research of artificial intelligence for deterministic solar power forecasting," *Energy Conversion and Management*, vol. 214, 2020.

[11] X. Liu, *et al.*, "A Hybrid AC/DC Microgrid and its Coordination Control," *IEEE Trans. Smart Grid*, vol. 2, no. 2, pp. 278–286, 2011.

[12] H. Wang, *et al.*, "Deep belief network based deterministic and probabilistic wind speed forecasting approach," *Applied Energy*, vol. 182, 2016, pp. 80-93;

[13] D. E. Olivares, *et al.*, "Trends in Microgrid Control," *IEEE Trans. Smart Grid*, vol. 5, no. 4, pp. 1905–1919, 2014.

[14] J. M. Guerrero, *et al*., "Advanced Control Architectures for Intelligent Microgrids - part I: Decentralized and Hierarchical Control," *IEEE Trans. Ind. Electron.*, vol. 60, no. 4, pp. 1254–1262, 2013.

[15] X. Huang, *et al.*, "Decentralized Control of Multi-Parallel Grid-Forming DGs in Islanded Microgrids for Enhanced Transient Performance," *IEEE Access*, vol. 7, pp. 17958-17968, 2019.

[16] M. S. Golsorkhi and D. D. C. Lu, "A Decentralized Control Method for Islanded Microgrids under Unbalanced Conditions," *IEEE Trans. Power Deliv.*, vol. 31, no. 3, pp. 1112–1121, 2016.

[17] S. Haider, *et al.*, "A dual control strategy for power sharing improvement in islanded mode of AC microgrid," *Prot Control Mod Power Syst* vol. 3, no. 10, 2018.

[18] F. Katiraei and M. R. Iravani, "Power Management Strategies for a Microgrid With Multiple Distributed Generation Units," *IEEE Trans Power Systems.*, vol. 21, no. 4, pp. 1821-1831, Nov. 2006.

[19] T. Kerdphol, *et al.*, "Robust Virtual Inertia Control of a Low Inertia Microgrid Considering Frequency Measurement Effects," *IEEE Access*, vol. 7, pp. 57550-57560, 2019.

[20] M. Yazdanian and A. Mehrizi-Sani, "Distributed Control Techniques in Microgrids," *IEEE Trans Smart Grid*, vol. 5, no. 6, pp. 2901-2909, Nov. 2014.

[21] M. Hamzeh, *et al.*, "Robust Control of an Islanded Microgrid Under Unbalanced and Nonlinear Load Conditions," *IEEE J. Emerg. Sel. Top. Power Electron.*, vol. 4, no. 2, pp. 512–520, 2016.

[22] L. Meng, *et al.*, "Distributed Voltage Unbalance Compensation in Islanded Microgrids by Using a Dynamic Consensus Algorithm," *IEEE Trans. Power Electron.*, vol. 31, no. 1, pp. 827–838, 2016.

[23] B. Liu, *et al.*, "An Adaptive Virtual Impedance Control Scheme Based on Small-AC-Signal Injection for Unbalanced and Harmonic Power Sharing in Islanded Microgrids," *IEEE Trans. Power Electron.*, vol. 8993, 2019.

[24] Y. Han, *et al.*, "An Enhanced Power Sharing Scheme for Voltage Unbalance and Harmonics Compensation in an Islanded AC Microgrid," *IEEE Trans. Energy Conversion.*, vol. 31, no. 3, pp. 1037-1050, Sept. 2016.

[25] A. Ranjbaran and M. Ebadian, "A Power Sharing Scheme for Voltage Unbalance and Harmonics Compensation in an Islanded Microgrid," *Electric Power Systems Research*, vol. 155, pp. 153- 163, 2018.

[26] Mohammad Hadi Andishgar, Mehdi Gholipour, Rahmat-allah Hooshmand, "Improved Secondary Control for Optimal Unbalance Compensation in Islanded Microgrids with Parallel DGs," *International Journal of Electrical Power & Energy Systems*, vol. 116, 105535, March. 2020.

[27] T. Jin, *et al.*, "Model Predictive Voltage Control Based on Finite Control Set with Computation Time Delay Compensation for PV Systems," *IEEE Trans. Energy Convers.*, vol. 34, no. 1, pp. 330–338, 2019.

[28] M. Tomlinson, *et al.*, "A Fixed Switching Frequency Scheme for Finite-Control-Set Model Predictive Control-Concept and Algorithm," *IEEE Trans. Ind. Electron.*, vol. 63, no. 12, pp. 7662–7670, 2016.

[29] S. Kouro, *et al.*, "Model predictive control - A Simple and Powerful Method to Control Power Converters," *IEEE Trans. Ind. Electron.*, vol. 56, no. 6, pp. 1826–1838, 2009.

[30] S. Vazquez, *et al.*, "Model Predictive Control for Power Converters and Drives: Advances and Trends," *IEEE Trans. Ind. Electron.*, vol. 64, no. 2, pp. 935–947, 2017.

[31] H. Miranda, *et al.*, "Predictive Torque Control of Induction Machines based on State-space Models," *IEEE Trans. Ind. Electron.*, vol. 56, no. 6, pp. 1916–1924, 2009.

[32] Y. Luo and C. Liu, "A Flux Constrained Predictive Control for a Six-phase PMSM Motor with Lower Complexity," *IEEE Trans. Ind. Electron.*, vol. 66, no. 7, pp. 5081–5093, 2019.

[33] P. Cortés, *et al.*, "Model Predictive Control of an Inverter with Output LC Filter for UPS Applications," *IEEE Trans. Ind. Electron.*, vol. 56, no. 6, pp. 1875–1883, 2009.

[34] Y. Zhang, *et al.*, "Fast Model Predictive Control for Multilevel Cascaded H-Bridge STATCOM with Polynomial Computation Time," *IEEE Trans. Ind. Electron.*, vol. 63, no. 8, pp. 5231–5243, 2016.

[35] M. R. Nasiri, *et al.*, "Model Predictive Control of a Multilevel CHB STATCOM in Wind Farm Application Using Diophantine Equations," *IEEE Trans. Ind. Electron.*, vol. 66, no. 2, pp. 1213–1223, 2019.

[36] M. G. Judewicz, *et al.*, "Generalized Predictive Current Control (GPCC) for Grid-Tie Three-Phase Inverters," *IEEE Trans. Ind. Electron.*, vol. 63, no. 7, pp. 4475–4484, 2016.

[37] M. S. Golsorkhi, and D. D. C. Lu, "A Decentralized Control Method for Islanded Microgrids under Unbalanced Conditions," *IEEE Trans. Power Delivery,* vol. 31, no. 3, pp. 1121-1121, June 2016.

[38] J. Liu, Y. Miura, and T. Ise, "Cost-Function-Based Microgrid Decentralized Control of Unbalance and Harmonics for Simultaneous Bus Voltage Compensation and Current Sharing," *IEEE Trans. Power Electron.,* vol. 34, no. 8, pp. 7397 - 7410, Aug. 2019.

[39] V. Yaramasu, *et al.*, "Model Predictive Approach for a Simple and Effective Load Voltage Control of Four-leg Inverter with an Output LC Filter," *IEEE Trans. Ind. Electron.*, vol. 61, no. 10, pp. 5259–5270, 2014.

[40] G. S. Perantzakis, *et al.*, "Efficient Predictive Current Control Technique for Multilevel Voltage Source Inverters," *2005 Eur. Conf. Power Electron.* Appl., pp. 1–10, 2005.

[41] H. A. Young, V. A. Marin, C. Pesce and J. Rodriguez, "Simple Finite-Control-Set Model Predictive Control of Grid-Forming Inverters With LCL Filters," *IEEE Access*, vol. 8, pp. 81246-81256, 2020.

[42] Y. Zhang, *et al.* "Hybrid Control Strategy of MPC and DBC to Achieve a Fixed Frequency and Superior Robustness," *Energies*, vol. 13, no. 5, 1176

[43] Z. Yi, *et al.*, "Finite-Control-Set Model Predictive Control (FCS-MPC) for Islanded Hybrid Microgrids," *2018 IEEE Power & Energy Society General Meeting (PESGM)*, Portland, OR, 2018, pp. 1-5.

[44] T. Dragicevic, "Model Predictive Control of Power Converters for Robust and Fast Operation of AC Microgrids," *IEEE Trans. Power Electron.*, vol. 33, no. 7, pp. 6304–6317, 2018.

[45] T. Dragičević, C. Zheng, J. Rodriguez and F. Blaabjerg, "Robust Quasi-Predictive Control of LCL-Filtered Grid Converters," *IEEE Trans. Power Electron*, vol. 35, no. 2, pp. 1934-1946, Feb. 2020.

[46] A. J. Babqi and A. H. Etemadi, "MPC-based microgrid control with supplementary fault current limitation and smooth transition mechanisms," *IET Generation, Transmission & Distribution*, vol. 11, no. 9, pp. 2164-2172, 22 6 2017.

[47] Toman, Riyadh T., and J. A. Asumadu, "Control of a Radial Micro-grid with Unbalanced Loads based on a Distributed Model Predictive Control for Grid Mode Operation," *2016 IEEE International Conference on Electro Information Technology (EIT) IEEE*, 2016.

[48] J. He, *et al.*, "An Enhanced Islanding Microgrid Reactive Power, Imbalance Power, and Harmonic Power Sharing Scheme," *IEEE Trans. Power Electron.*, vol. 30, no. 6, pp. 3389–3401, 2015.

This article has been accepted for publication in a future issue of this journal, but has not been fully edited. Content may change prior to final publication. Citation information: DOI 10.1109/ACCESS.2020.3034947, IEEE Access

Author Name: Preparation of Papers for IEEE Access

ZHUOLI ZHAO (S'15–M'18) received the B.S. degree and the Ph.D. degree from South China University of Technology, Guangzhou, China, in 2010 and 2017, respectively.

From October 2014 to December 2015, he was a Joint Ph.D. Student (Sponsored Researcher) with the Control and Power Research Group, Department of Electrical and Electronic Engineering, Imperial College London, London, U.K. He was a Research Associate with the Smart Grid Research Laboratory, Electric Power Research Institute, China Southern Power Grid, Guangzhou, China, from 2017 to 2018.

He is currently an Associate Professor with the School of Automation, Guangdong University of Technology, Guangzhou, China. His research interests include microgrid control and energy management, power electronic converters, smart grids, and distributed generation systems. He is an Active Reviewer for the IEEE Transactions on Power Electronics, the IEEE Transactions on Smart Grid, the IEEE Transactions on Sustainable Energy, the IEEE Transactions on Industrial Electronics, the IEEE Access and the Applied Energy.

JIEXIONG ZHANG received the B.Eng. degree from Guangdong University of Technology, Guangzhou, China, in 2018.

He is currently working toward the master degree in electrical engineering with the School of Automation, Guangdong University of Technology, Guangzhou, China. His research interests include microgrid control and power electronics.
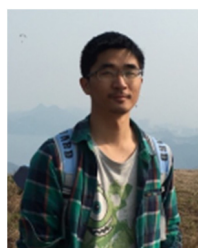
BAIPING YAN received his M.S. and Ph.D. degree from Harbin Institute of Technology, Harbin, China, in 2009 and 2014, respectively.

Currently, he is an Associate Professor with the School of Automation, Guangdong University of Technology, Guangzhou, China. His research interests include power electronics and electric drives, intelligent electromagnetic structure and devices.

RUNTING CHENG received the B.Eng. degree in electrical engineering and automation from the Northeast Forestry University, Harbin, China, in 2018.

She is currently working toward the master degree in electrical engineering with the School of Automation, Guangdong University of Technology, Guangzhou, China. Her research interests include maximum power point tracking technology, power electronic converters, and distributed generation systems.

CHUN SING LAI (S'11–M'19) received the B.Eng. (First Class Honours) in electrical and electronic engineering from Brunel University London, UK and D.Phil. in engineering science from the University of Oxford, UK in 2013 and 2019, respectively.

Dr Lai is currently a Lecturer at Department of Electronic and Computer Engineering, Brunel University London, UK and also a Visiting Academic with the Department of Electrical Engineering, Guangdong University of Technology, China. He is a member of Brunel Institute of Power Systems. From 2018 to 2020, he was an Engineering and Physical Sciences Research Council Research Fellow with the School of Civil Engineering, University of Leeds. He is Secretary of the IEEE Smart Cities Publications Committee and Acting EiC of IEEE Smart Cities Newsletters. He organized the workshop on Smart Grid and Smart City, IEEE SMC 2017 in Canada. Dr Lai is the Working Group Chair for IEEE P2814 Techno-economic Metrics Standard for Hybrid Energy and Storage Systems.

LIPING HUANG (S'16) received the B.Eng. degree from the China University of Mining and Technology, Beijing, China, in 2016. She is currently pursuing the Ph.D. degree with the School of Automation, Guangdong University of Technology, Guangzhou, China. She is now a visiting Ph.D. student with the Center for Electric Power and Energy, Department of Electrical Engineering, Technical University of Denmark. Her research interests are in power system optimal operation and control, reliability, and resilience evaluation.

QUANXUE GUAN (S'11, M'16) received his B.S. degree in Automation Engineering from the South China University of Technology (SCUT), Guangzhou, China, in 2007. He started his combined M.Sc./PhD program in Control Theory and Control Applications since 2009 and received his PhD degree in Power Electronics and Motor Drives from the South China University of Technology, Guangzhou, China, in 2016. He was a Project Engineer with HILTI (China) Ltd., Zhanjiang, China, during 2007-2008. In 2016, he joined the School of Electronics and Information Technology, Sun Yat-sen University, Guangzhou, China, as a Research Associate. In 2017, he joined, as a Research Fellow, the Power Electronics and Motor Control group, University of Nottingham, UK, where he visited during 2013-2014. His current research interests include matrix converters, dual-active-bridge DC/DC converters, wide band-gap (GaN/SiC) power devices and applications, and advanced energy management in more electric aircrafts.

LOI LEI LAI (M'87–SM'92–F'07) received B.Sc. in 1980, Ph.D. in 1984 and D.Sc. in 2005 from University of Aston and City, University of London respectively.

Presently he is University Distinguished Professor at Guangdong University of Technology, Guangzhou China. He was a member of the IEEE Smart Grid Steering Committee; Director of Research and Development Centre, State Grid Energy Research Institute, China; Pao Yue Kong Chair Professor at Zhejiang University, China; Vice President with IEEE Systems, Man and Cybernetics Society (IEEE/SMCS); Professor & Chair in Electrical Engineering at City, University of London; and a Fellow Committee Evaluator for IEEE Industrial Electronics Society. He was awarded an IEEE Third Millennium Medal, IEEE Power and Energy Society (IEEE/PES) UKRI Power Chapter Outstanding Engineer Award in 2000, IEEE/PES Energy Development and Power Generation Committee Prize Paper in 2006 & 2009, IEEE/SMCS Outstanding Contribution Award in 2013 & 2014 and the Most Active Technical Committee Award in 2016. He is a member of the IEEE Smart Cities Steering Committee, a Fellow of IET and IEEE & National Distinguished Expert in China and Distinguished Expert in State Grid Corporation of China.